05

Technique for investigation of the shape changes of wafers and thin-film membranes by using geomorphometric approaches

© A.A. Dedkova,[1,2] I.V. Florinsky,[2] N.A. Djuzhev[1]

[1] National Research University of Electronic Technology,
124498 Zelenograd, Moscow, Russia
[2] Institute of Mathematical Problems of Biology, Keldysh Institute of Applied Mathematics, Russian Academy of Sciences,
142290 Pushchino, Russia
e-mail: dedkova@ckp-miet.ru, iflor@mail.ru

We discuss a technique for investigating changes in complex topography and shape of structures using geomorphometric methods to study surfaces of wafers and membranes formed by the Bosch process. The wafers were analyzed before and after the deposition of the SiO_2 layer. The membranes were analyzed during the bulge testing. The study was carried out using maps of the catchment area and principal curvatures taking into account artifacts of the approximation of experimental data. We found a correspondence between the distribution of lines connecting the highest surface areas before and after the deposition of the SiO_2 layer on the wafers. For membranes with structure: $Al(0.8\,\mu m)/SiO_2(0.6\,\mu m)/Al(1.1\,\mu m)$, $pSi^*(0.8\,\mu m)/SiN_x(0.13\,\mu m)/SiO_2$, $Al(0.6\,\mu m)$ we also found that features of membrane boundaries are mainly caused by their initial shape rather than change under the action of an applied pressure. The advantages of geomorphometric methods for studying changes in the shape of wafers and thin-film membranes in technological processes for the manufacturing of microelectronic devices are shown in comparison with traditional methods for analyzing surface topography maps.

Keywords: thin films, membrane, defect, mechanical characteristics, mechanical stresses, deformation, deflection, strain, microelectromechanical systems, MEMS, circular membrane, silicon substrate, optical profilometry, overpressure, geomorphometry, Gaussian curvature, warpage, principal curvatures, wafer, bulge testing, bulging method, thin-layer coating, digital elevation models, DEM, surface, topography.

Introduction

Methods for studying changes in the shape and topography of the surface of semiconductor wafers and structures are in demand for the microelectronic industry. For an effective comprehensive qualitative and quantitative assessment of the topographic features, a digital elevation model (hereinafter — DEM) of the surface of structures should be constructed and analyzed. It is proposed to use a complete system of surface curvature based on the methods of geomorphometry [1,2] to study the features of the topography.

Such studies of complex forms of structures based on DEM are necessary in various fields:

1. In microelectronic production, when carrying out technological processes for processing wafers in order to form microelectronic devices and systems from them, warpage (flatness change) of wafers, mechanical stresses and deformations are observed. These stresses and deformations reduce the reliability of microelectronic devices and systems, and warpage of wafers causes problems with their clamping and transportation in technological equipment. A detailed study of the warpage process of wafers is caused by the growing requirements for the characteristics of structures and the need to ensure sufficient strength for their functioning. Uneven stress and deformation, significant influence of the method and area of wafer attachment, the influence of gravity [3] — becomes much more pronounced for wafers with a diameter of 300 mm [4], for thinned wafers [5], including when creating wafer assemblies [6]. Separately, it should be noted that with a decrease in the thickness of the wafers, an asymmetric (cylindrical, saddle-shaped) bend begins to be observed [4,7,8], this process is currently poorly understood. To reduce the warpage of the wafers, heat treatment can be used, applying a film to the back of the wafer [7], forming compensating structures on the back of the wafer [7], controlling the thickness and mechanical stresses of the layers, etc. [9]. In order to understand the warpage process and combat its consequences, comprehensive information is needed about the peculiarities of surface topography changes.

2. In X-ray optics, to create reflective elements — aspherical surfaces [10–18]. One of the most important characteristics determining the resolution and lens speed of X-ray mirrors is the accuracy of the shape of the manufactured surface [16]. The use of aspherical surfaces is complicated by the difficulties of their manufacture and control due to the variability of the radius of curvature of the item. The study [18] describes in detail the method of aspherization of the surface, experimental and calculated profiles of the deviation of the surface from the sphere, a map of the deviation of the surface shape. However, in such

works, a complete system of surface curvature is not used, which could significantly improve the control of the shape of the surface and analyze its changes.

3. In mechanical engineering. When forming the surfaces of items, the analysis and classification of surface shapes are common. To successfully solve the problems of optimizing the processing of complex parts on numerically controlled machines during the development of the technological process, the representation and parameterization of free-form surfaces [19–21] is required.

4. In a detailed study of the surface topography and shape of MEMS structures and products based on them: accelerometers [22], pressure sensors [23], adaptive optics [24,25] and others. Here it is necessary to analyze both the initial form of MEMS and its change, both under the influence of the expected functionally necessary influences [25], and under the influence of various destructive factors [26].

The present work is devoted to the development and use of a geomorphometry-based methodology designed to study changes in the complex shape of wafers and thin-film membranes formed in the technological processes of microelectronic production.

The described technique is intended for a more detailed study of the surface topographic features in comparison with standard methods of topographic map analysis. The technique allows us to distinguish a variety of weakly pronounced features of the topography, which will allow us to draw conclusions about certain technological processes and properties of the emerging structures in the future.

1. Geomorphometric methods

Geomorphometry is a scientific discipline, the subject of which is mathematical modeling and analysis of topography, as well as the relationships between it and other components of geosystems.   Currently, geomorphometry is widely used to solve problems of geomorphology, hydrology, soil science, geobotany, geology, glaciology, oceanology, climatology and other Earth sciences [1].

A morphometric variable is an unambiguous function of two variables describing the properties of a topographic surface.   The list of variables used in geomorphometry, which are calculated according to the DEM, includes, in particular, the following 12 curvatures, which make up the complete system of curvatures [1,2]: horizontal curvature, vertical curvature, difference curvature, horizontal excess curvature, vertical excess curvature, accumulative curvature, ring curvature, minimum curvature, maximum curvature, mean curvature, Gaussian curvature, unsphericity. Their formulas and brief interpretations are given in [1,2,30]. Each of these variables has its own physical and mathematical meaning, describing a particular feature of the local geometry of the surface. A complete system of curvatures is understood as the mathematical completeness of a system of variables. A comprehensive description of the topographic

features of an object is possible only when using digital models of all these 12 variables derived from DEMs [1]. The list of morphometric variables is not limited to this list, it also includes the catchment area, slope aspect (orientation), slope steepness, etc. [1].

2. Equipment and calculations

To form digital elevation models, the Veeco Wyko NT 9300 optical profilometer was used, forming DEMs of structures with a diameter of up to 200 mm, with a resolution from 98 nm to $57\,\mu$m.   When analyzing the wafers, the resolution was reduced to $\sim 0.5\,$mm.   When analyzing membranes, the size of the DEM matrix was 640×480, resolution $\sim 4\,\mu$m.

A universal spectral analytical method using Chebyshev polynomials and Feyer summation [31] was used to calculate morphometric variables. The method is designed to process regular DEMs within a single scheme, including global approximation of the DEM, generalization and noise suppression in the DEM, as well as the calculation of morphometric characteristics based on the analytical calculation of partial derivatives.   The approximation is characterized by monotonic convergence and the possibility of rapid deep decomposition of the elevation function (up to 7000 decomposition coefficients n; the total number of decomposition coefficients is n^2, since the function decomposes into the same number of decomposition coefficients along two planimetric coordinates).

Morphometric variables are usually characterized by a wide dynamic range of values.   To avoid the loss of information about their spatial distribution, a logarithmic transformation of the following form is used for the mapping [1,30]:

$$\tilde{\Upsilon} = \text{sign}(\Upsilon)\ln\bigl(1 + 10^{\hat{n}\hat{m}}|\Upsilon|\bigr), \qquad (1)$$

$\tilde{\Upsilon}$ and Υ are the transformed and original values of the morphometric variable, respectively; $\hat{n} = 0$ for non-local variables, $\hat{n} = 2, \dots, 9$ for local variables; $\hat{m} = 2$ for K, K_a and K_r, $\hat{m} = 1$ for other variables. The choice of the value $\hat{n}$ depends on the grid size of the DEM.

3. Samples

To demonstrate the possibility of studying wafers with deposited films on the maps of the catchment area, silicon (Si) wafers with a diameter of 100 mm were used (Figs. 1, 2). The formation of silicon oxide (SiO_2) was carried out on these wafers: a thickness of $0.6\,\mu$m (PlasmalabSystem installation 100 (Oxford), $T = 100°$C, RF generator 150 W, ICP 300 W, N_2O 80 cm^3/min, SiH_4 34 cm^3/min, $P = 4\,$mTorr, $t = 20\,$min).

To demonstrate the analysis of MEMS structures, thin-film membranes formed by the Bosch process [32–34] were studied (Figs. 3−6). The membranes were created from
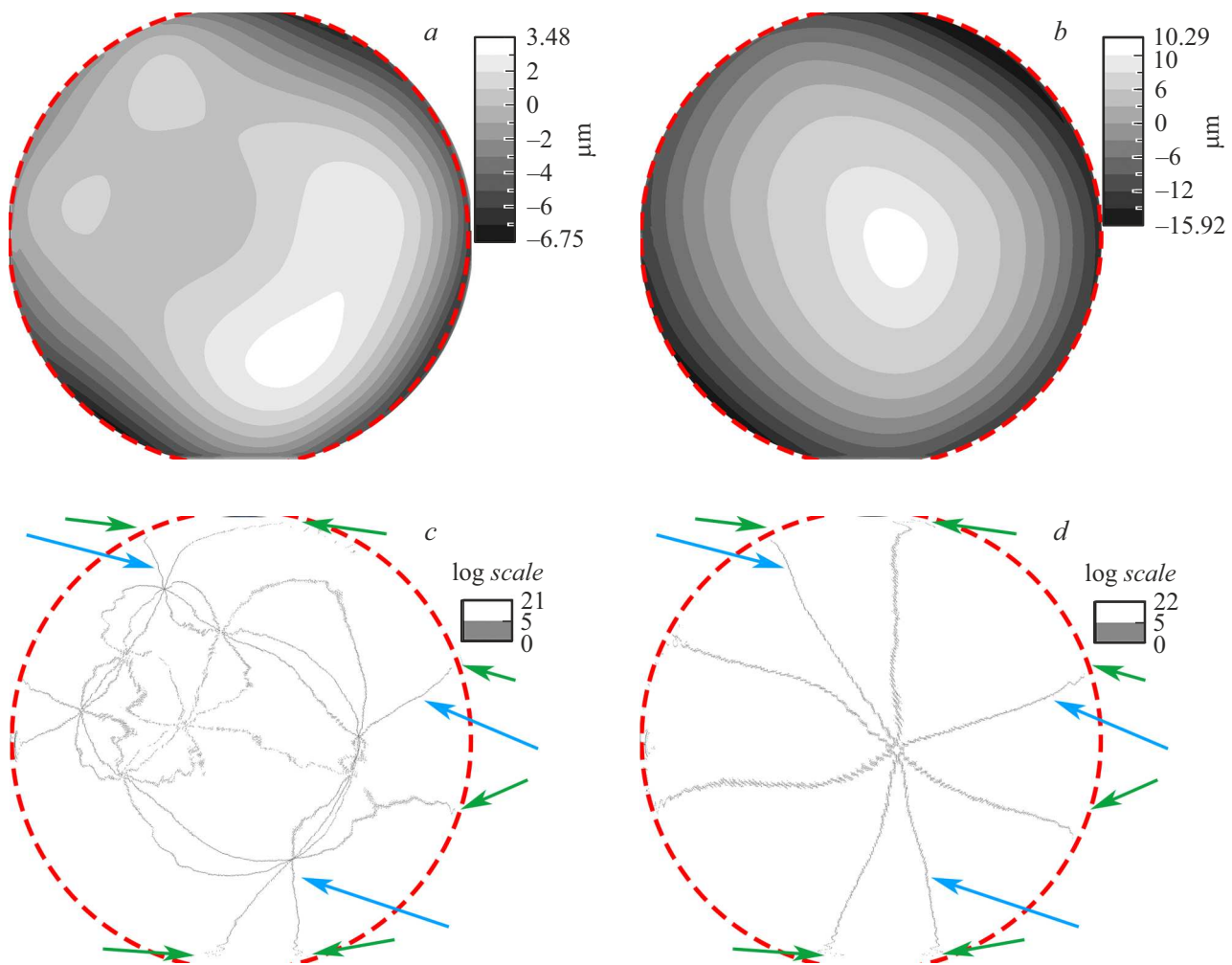
Figure 1. Sample №1: surface topography before (a) and after (b) formation of the SiO$_2$ layer, catchment area (binary map) before (c) and after (d) formation of the SiO$_2$ layer.

thin films preformed on the front side of the silicon wafer, after deep through anisotropic etching of silicon from the back side of the wafer in the Bosch process to the film (Fig. 3). In the research process, various membranes were analyzed, the most typical and illustrative cases are presented in Figs. 3−6:

— initially stretched membrane with a small initial deflection w — about $3\,\mu$m (Figs. 3,4), structure pSi*$(0.8\,\mu$m)/SiN$_x$$(0.13\,\mu$m)/SiO$_2$$(0.5\,\mu$m);

— membrane with small folds and initial deflection w less than $1\,\mu$m (Fig. 5), structure: 20 layers Al with a total thickness of $0.6\,\mu$m by using ion bombardment after deposition of each layer;

— membrane with significant folds and initial deflection w more than $30\,\mu$m (Fig. 6), structure Al$(0.8\,\mu$m)/SiO$_2$$(0.6\,\mu$m)/Al$(1.1\,\mu$m).

The membranes were studied during the implementation of the bulge testing. This procedure is used to determine the mechanical characteristics of films and structures. The method consists in fixing the edges of the membrane along the perimeter, applying (one-sided) overpressure to it from one side, analyzing the dependence of the deflection of the membrane on the value of the applied overpressure, calculating the elastic modulus or other values [35–39]. Since the membranes formed by the Bosch process differ in the presence of an initial deflection and a complex shape even before the overpressure is applied, the study of their stress-strain state requires detailed consideration [32,33].

4. Investigation of changing the shape of wafers with films

Earlier, the authors described in detail the studies of the local shape features of wafers with films using Gaussian, mean and principal curvatures [27–29]. To study the process of changing the shape of wafers during the formation of films of various materials on their surface, it is also useful to use other morphometric variables.

Prior to the technological processes, the initial surfaces of silicon wafers with an average standard thickness of $650\,\mu$m can be considered quite flat, since the deflection usually

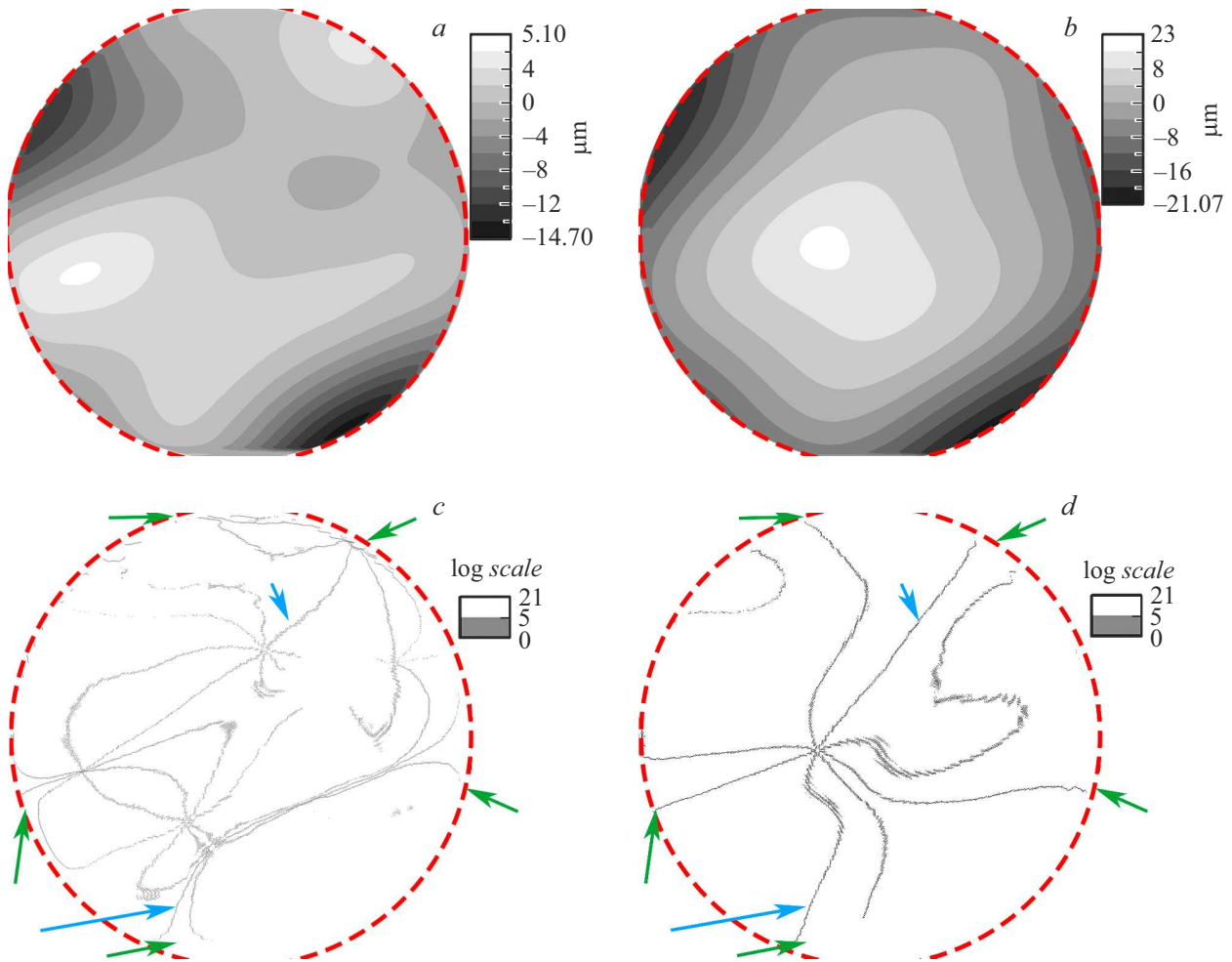**Figure 2.** Sample №2: surface topography before (*a*) and after (*b*) formation of the SiO$_2$ layer, catchment area (binary map) before (*c*) and after (*d*) formation of the SiO$_2$ layer.
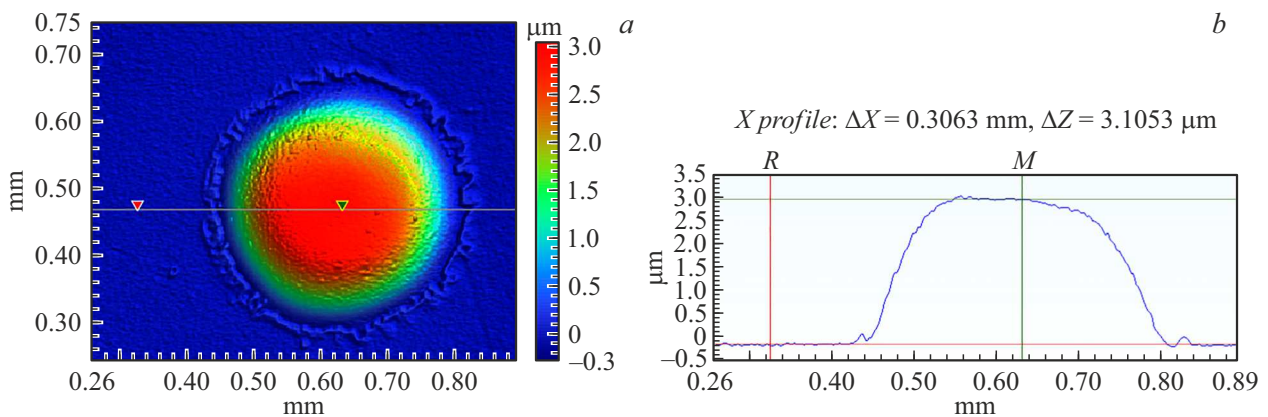

Figure 3. The original shape of the membrane pSi*(0.8 μm)/SiN$_x$(0.13 μm)/SiO$_2$(0.5 μm): *a* — surface topography (DEM), *b* — surface profile along the drawn line. On surface topography maps here and further the color scale is from blue (lowest value) to red (highest value (color in online version)).

does not exceed several micrometers. The application of a functional layer (film) to the surface of the wafer leads to a curvature of the formed structure „substrate and layer", the shape of which is often close to spherical [40]. In reality, the initial shape of silicon wafers is complex, which also affects the shape of the formed structure „Si-wafer and layer".

Figs. 1, 2 present data on two Si-wafers with a diameter of 100 mm with SiO$_2$ thickness of 0.6 μm before and after
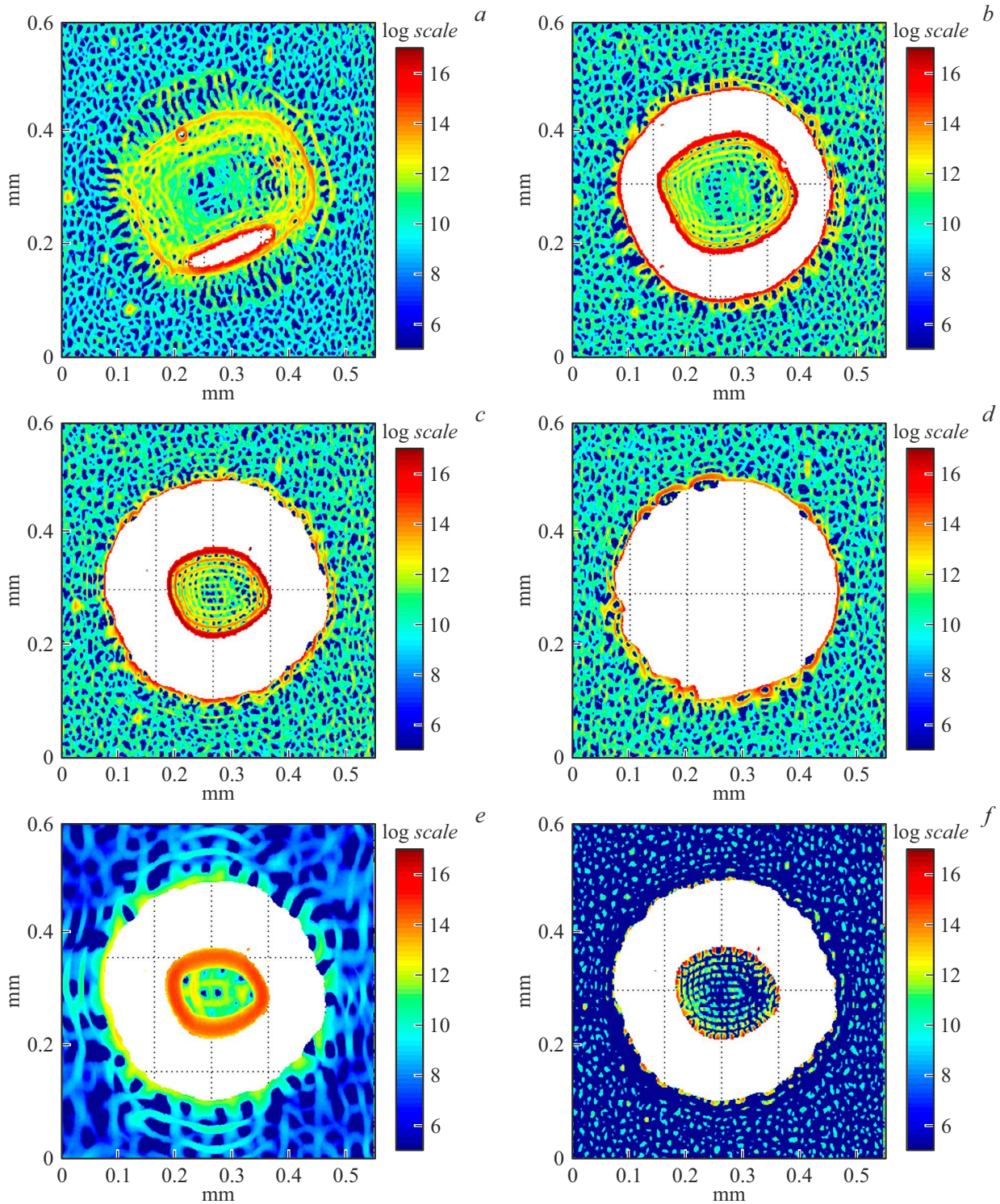
Figure 4. Membrane $pSi^*(0.8\,\mu m)/SiN_x(0.13\,\mu m)/SiO_2(0.5\,\mu m)$: a — k_{max} ($P = 0$, slight compression; $w = 4.1\,\mu m$), b — k_{max} ($P = 0.8\,atm$; $w = 6.8\,\mu m$), c — k_{max} ($P = 3.6\,atm$; $w = 10.6\,\mu m$), d — k_{max} (after separation), e — k_{max} ($P = 3.6\,atm$; $w = 10.6\,\mu m$), f — k_{min} ($P = 3.6\,atm$; $w = 10.6\,\mu m$). When approximating $n = 300$ (a–d,f), $n = 100$ (e).

the formation of the layer. The thickness of the layers was monitored using a Horiba Uvisel 2 spectral ellipsometer.

Despite the relatively close shape of the wafers with films to the spherical segment (Figs.1, b and 2, b), they contain patterns (topographic features that fit into the pattern-

image), interconnected with the patterns of the original DEM before formation of the layer (Figs. 1, a and 2, a). In particular, the distribution of the highest areas of the surface of the — analog of „ridges" correlates. It is convenient to analyze such distributions using catchment
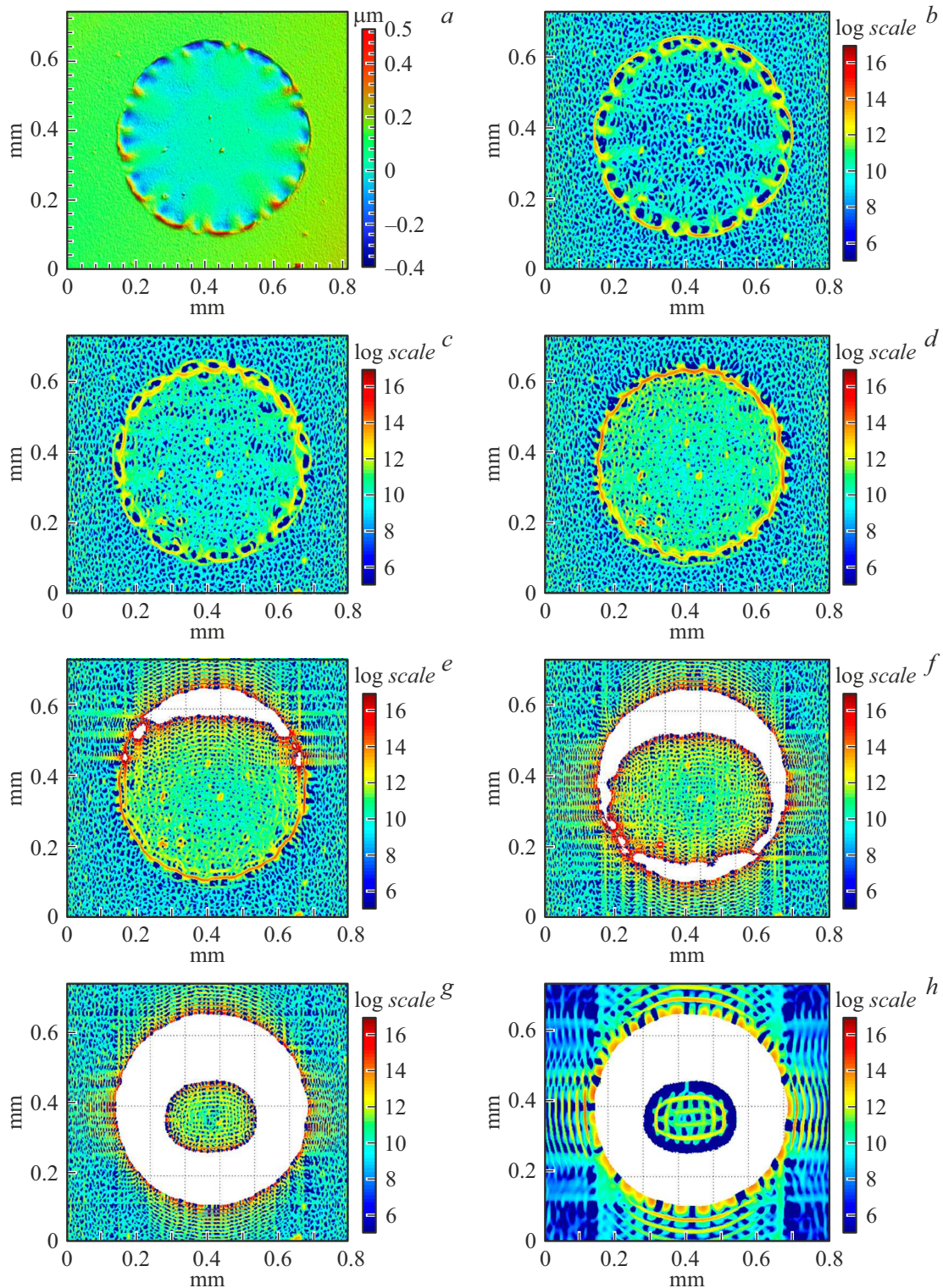
Figure 5. Membrane Al $(0.6\,\mu m)$: a — topography ($P = 0$ atm; $w = -0.13\,\mu m$), b — k_{max} ($P = 0$ atm; $w = -0.13\,\mu m$), c — k_{max} ($P = 0.3$ atm; $w = 1.8\,\mu m$), d — k_{max} ($P = 0.6$ atm; $w = 3.9\,\mu m$), e — k_{max} ($P = 0.9$ atm; $w = 5.9\,\mu m$), f — k_{max} ($P = 1.2$ atm; $w = 7.6\,\mu m$), g, h — k_{max} ($P = 2.5$ atm; $w = 13.8\,\mu m$). When approximating $n = 300$ (b–g), $n = 100$ (h).

area maps. For these structures, they are shown in Figs. 1, c, d and 2, c, d. The calculation was carried out on the basis of one of the flow routing algorithms — the Martz-De Young method [30]. The catchment area is the

area of a closed figure formed by a segment of a contour line (which includes this point) and two flow lines coming from the overlying point. Since there are the smallest number of overlying areas on the „ridges", this leads to the fact that the
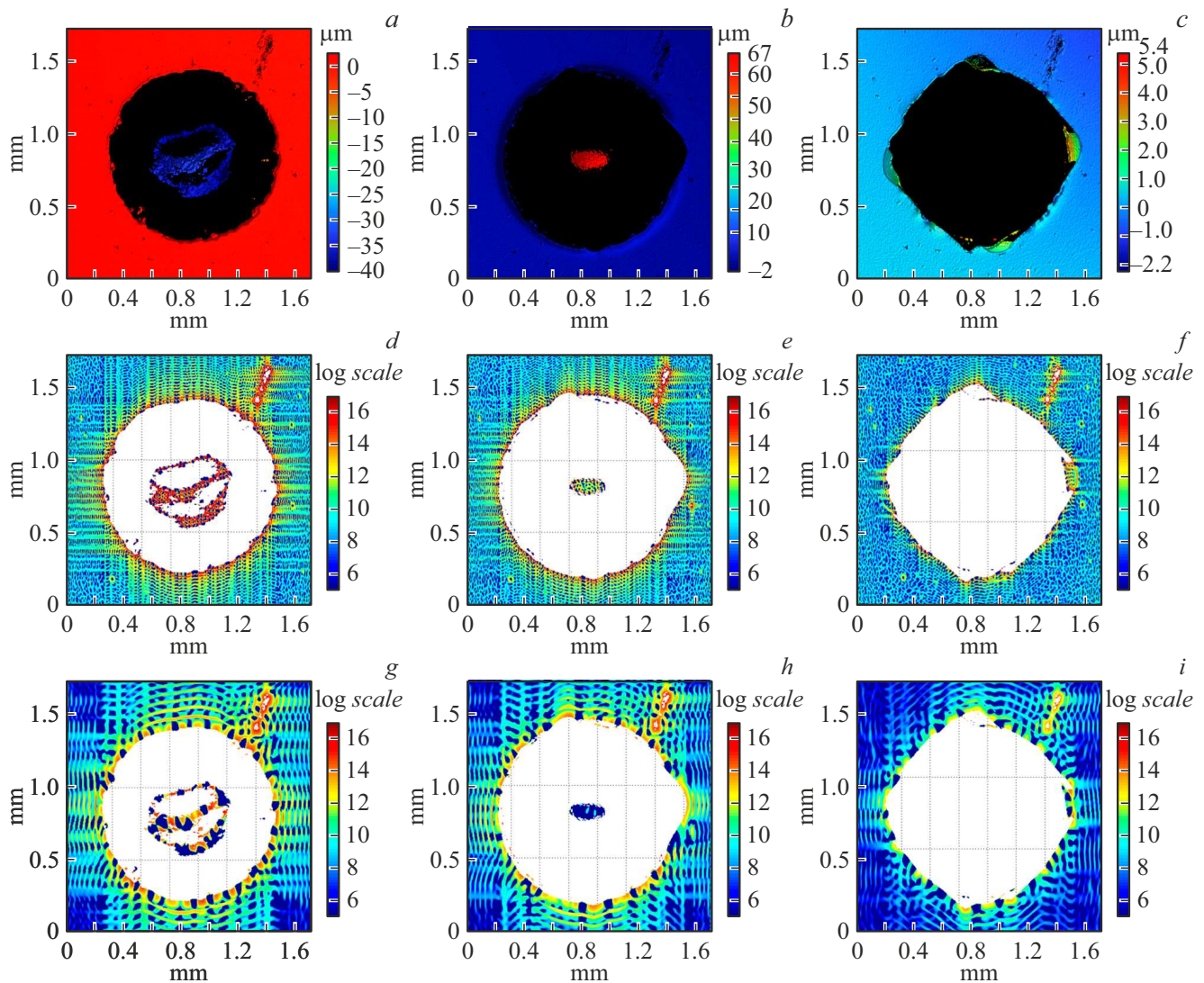
Figure 6. Membrane $Al(0.8\,\mu m)/SiO_2(0.6\,\mu m)/Al(1.1\,\mu m)$: a–c — topography; d–f — k_{max} ($n = 300$); g–i — k_{max} ($n = 100$). Shown: a, d, g — the original membrane ($P = 0$ atm; $w = -40\,\mu m$); b, e, h — pressurized membrane ($P = 2.8$ atm; $w = 66\,\mu m$); c, f, i — after membrane separation.

smallest values of the catchment area visualize their location (which is most clearly manifested when constructing a binary map).

The position of the lines of the „ridges" before and after application of the layer is consistent: the position of the lines closer to the edge of the wafer mostly coincides, and in some cases the position of the lines along the main area of the wafer is correlated (shown by the arrows in Figs. 1, c, d and 2, c, d). A similar effect is observed when analyzing maps of slope aspect, maximum curvature, etc.

Thus, the use of the methodology for analyzing the features of the topography using geomorphometric methods for the study of structures, namely, to determine the location of the lines connecting the highest points of the surface, is shown. This information can be useful for understanding the mechanism of deformation of the wafer and predicting

its actual shape after the technological processes carried out.

It is also shown that the study of the topographic features of wafers with films formed on their surface using an analysis technique based on geomorphometric methods, in contrast to standard DEM analysis techniques (when analyzing only topographic maps obtained by optical profilometry or another method) makes it possible to determine the location of lines connecting the highest points of the surface. This information is very important for developers of microelectronic devices and technologists to understand the mechanism of deformation of wafers with structures and predict their real shape after the technological processes carried out. Changing the location of these lines during the thinning of the wafers (the transition of the bend to the saddle) can allow a deeper understanding of the warpage process and control it.

5. Investigation of the shape change of thin-film membranes

The methods of studying the DEM of small objects, including MEMS structures, are generally similar to the method of studying wafers. However, when working with the DEM of thin-film membranes, including membranes with an initial deflection, and membranes in the process of bulge testing, there is an important feature: the fact that there are areas without data in the analyzed DEM (Figs. 4–6) caused by too large an angle of inclination of these areas [32,34].

If there is no data in the DEM for its processing, such areas are usually filled with certain values (for example, zeros), and then after the calculations, the data from these areas on the calculated maps are deleted again. This approach works in the case of a sufficiently small area of such regions, however, when analyzing the DEM of curved membranes, they can make up a significant part of the DEM (Fig. 6, b).

Another option is to restore data to an initially empty area. However, this process is often difficult to accomplish. Not in all cases, it is possible to predict with certainty the shape of the membrane that cannot be determined experimentally. If there is an assumption, such restoration is lengthy and painstaking, while due to the presence of a sharp boundary between the membrane region and the substrate, certain artifacts caused by approximation or interpolation of such data (analogous to the Gibbs phenomenon [41]) will still be present on the maps of the calculated morphometric variables.

For this reason, it is proposed to analyze the DEM of membranes in the simplest way, while taking into account the features caused by the presence of areas without data.

Of greatest interest is the narrow data area— the area of membrane attachment to the substrate (along the perimeter of the membrane). The part of it available for analysis gradually decreases as the membrane is under overpressure. A series of membranes pSi*$(0.8\,\mu\text{m})$/SiN$_x$ $(0.13\,\mu\text{m})$/SiO$_2(0.5\,\mu\text{m})$ of various diameters was studied (hole diameters in the photomask from 250 to $1000\,\mu\text{m}$). After completion of the tests (separation of membranes), there were both relatively smooth holes left by destroyed membranes of large and medium diameters, withstanding pressure up to 3.7 atm, and holes with ragged edges left by destroyed membranes of small diameter, withstanding pressure of the order of 5 atm. Also, a „halo" around the membranes was observed on these structures (Fig. 3) — a small ring with a swollen film. The same „halo" is also visible on the map of maximum curvature $k_{\max}$ (Fig. 4, a). As the applied overpressure increases in the area inside the „halo" the maximum curvature of $k_{\max}$ increases. With an increase in the applied overpressure, separate closely located areas with sufficiently high values of $k_{\max}$ merge into one (Fig. 4, b, c). The minimum curvature ($k_{\min}$) also shows the local convex (most prominent) areas (Fig. 4, f).

Here and further it should be taken into account that such areas correspond to the greatest curvature, i.e. convex zones, which means the greatest deviation of the position of the structure from the plane of the substrate. This may be a consequence of the partial separation of the film from the substrate, but does not explicitly prove the presence of maximum mechanical stresses in this area. After the membrane separation, the distribution features of $k_{\max}$ correspond to the position and shape of the structure residues (Fig. 4, d).

Similar effects of gradual fusion of adjacent regions with high values of $k_{\max}$ were observed on membranes of different diameters from this batch of pSi*$(0.8\,\mu\text{m})$/SiN$_x(0.13\,\mu\text{m})$/SiO$_2(0.5\,\mu\text{m})$. However, when analyzing large-diameter membranes in the generated image, the area between the „halo" and the beginning of the absence of data is very narrow (including relative to the diameter of the membrane), which complicates the analysis and makes it less effective. Particularly, when analyzing a membrane with a diameter of 1 mm (separation occurred at $P = 2.6$ atm), no significant change in local curvature was detected. This may be both a consequence of the very absence of a change in the local curvature (which may indirectly indicate the features of the stress-strain state), and the inability of this technique to record such changes. For this reason, for such membranes, the described approach is proposed to be used in the analysis of structures of small diameter.

It was found that when using a low degree polynomial ($n = 100$), fragments of concentric circles are present on the calculated maps of $k_{\max}$ (Fig. 4, e). This is more noticeable on the membranes Al $(0.6\,\mu\text{m})$ (Fig. 5, h) and Al$(0.8\,\mu\text{m})$/SiO$_2(0.6\,\mu\text{m})$/Al$(1.1\,\mu\text{m})$ (Fig. 6, g–i). These artifacts (an analogue of the Gibbs phenomenon [41]) are a consequence of the features of the approximation process of the DEM.

The presence of such artifacts and their rounded shape on the curvature maps indicates the shape of the area without data close to the circle (which then leads to a smooth hole after the membrane is torn off). On the sample Al $(0.6\,\mu\text{m})$, such concentric circles are clearly visible, and after the separation of the membrane, a circular hole remains. Similar artifacts are visible on the sample Al$(0.8\,\mu\text{m})$/SiO$_2(0.6\,\mu\text{m})$/Al$(1.1\,\mu\text{m})$, but their shape is uneven — does not correspond to the circle, as well as the one formed after tear off the membrane hole.

Another common artifact is the „bands" of relatively high values of $k_{\max}$, observed, on the contrary, in areas where the shape of the border differs from a perfectly round one. From these bands, it can be concluded that there are irregularities (or defects) along the perimeter of the membrane (Figs. 5, e–h, 6, d–i). In fact, „bands" are an indicator of border irregularity (often characteristic of compressed membranes or membranes with folds). As the membrane is under overpressure, the adjacent „bands" merge (Fig. 6, d, e, g–h).

With a relatively small degree of approximation polynomial ($n = 100$), the corresponding maps of morphometric variables near the perimeter of the membrane reflect not so much the nature of the topography in the analyzed local areas themselves, as the nature of the boundary with the area without data (Figs. 4, e, 5, h, 6, g–i). With a higher degree of the polynomial ($n = 300$), such artifacts are also present, but they are less significant and almost do not interfere with the analysis of the topography near areas without data (Figs. 4, a–d, 5, e–g, 6, d–f).

It should be noted that on Al($0.6\,\mu$m) and Al($0.8\,\mu$m)/SiO$_2$($0.6\,\mu$m)/Al($1.1\,\mu$m) membranes there are defects of an uneven boundary membranes (causing „bands") were present initially (before applying overpressure). Artifacts appeared when areas without data appeared (Fig. 5, e). And on various membranes pSi*($0.8\,\mu$m)/SiN$_x$($0.13\,\mu$m)/SiO$_2$($0.5\,\mu$m), in connection with a more even border, „bands" almost not observed, including in the analysis of heavily pressurized membranes.

Consequently, the main character of the membrane boundary is more due to its shape at the initial membrane (before overpressure supply) than to the change under the action of the applied overpressure.

Nevertheless, the described technique makes it possible to analyze the change in the surface topography near the fixation of the membrane. Thus, Fig. 5, b–g shows a gradual shift in the position of the highest values of $k_{\max}$ (before loading — along the outer circle relative to the initial irregularities along the perimeter of the membrane, after loading — by the inner circle). Also, on Fig. 4, a and 5, d, extended regions of the smallest values of $k_{\max}$ are visible. They correspond to the area of local depressions, presumably caused by membrane tightening. In the case of Fig. 4, a, this may be the result of a slight compression in the holder when attached to the stand. In the case of Fig. 5, — a consequence of the loading of the membrane; with even greater overpressure, these regions of the lowest value of $k_{\max}$ are also present, but less clearly, due to the aforementioned artifacts.

Thus, the study of the features of the topography of membranes formed by films on the surface of silicon wafers using an analysis technique based on geomorphometric methods, in contrast to the standard analysis of topographic maps, makes it possible to visualize the location of convex and concave elements of the membrane surface at their boundary regions and to analyze the degree of evenness of the area of fixation and separation of the membrane. This allows us to make assumptions about the areas of separation of the film from the substrate. Since these changes are rather weakly expressed, they are practically not noticeable directly on the surface topography maps and cannot be detected using standard analysis methods.

Conclusion

The technique of surface topography analysis based on geomorphometric approaches that allow analyzing local surface features of structures in microelectronics is described. Using the example of silicon wafers with formed films and round thin-film membranes, it is shown that this technique will allow obtaining new information in comparison with standard methods for analyzing surface topography maps, namely:

1. Determine the location of the lines connecting the highest points of the surface of the wafers with the films. This makes it possible to identify patterns of inheritance of the original topography after the technological processes.

2. To visualize the location of convex and concave elements of the membrane surface at their boundary regions and analyze the degree of evenness of the region of fixation and separation of membranes. This technique allows us to study the process of changing the topography of the membrane surface and nearby areas.

This information is very important for developers of microelectronic devices and technologists to understand the mechanism of deformation of wafers with structures and predict their real shape after the technological processes carried out.

Funding

Acknowledgments

Conflict of interest

The authors declare that they have no conflict of interest.

References

[1] I.V. Florinsky *Digital Terrain Analysis in Soil Science and Geology. 2nd ed.* (Elsevier/Academic Press, Amsterdam, 2016)

[2] P.A. Shary. Mathematical Geology, **27** (3), 373 (1995). DOI: 10.1007/BF02084608

[3] H. Liu, Z Dong, R. Kang, P. Zhou, S. Gao. Metrol. Meas. Syst, **XXII** (4), 531 (2015). DOI: 10.1515/mms-2015-0052

[4] G.T. Ostrowicki, S.P. Gurum, A. Nangia. IEEE 68th Electron. Components and Technol. Conf., 2110 (2018). DOI: 10.1109/ECTC.2018.00317

[5] X. Zhu, X. Chen, H. Liu, R. Kang, B. Zhang, Z. Dong. Mater. Res. Express, **4**, 065904 (2017). DOI: 10.1088/2053-1591/aa71ed

[6] Y. Kim, S.-K. Kang, S.-D. Kim, S.E. Kim. Microelectron. Engineer., **89**, 46 (2012). DOI: 10.1016/j.mee.2011.01.079

[7] D. Shi, Z. Xia, M. Hu, G. Mei, Z. Huo. Semicond. Sci. Technol., **35** (4), 045031 (2020). DOI: 10.1088/1361-6641/ab73eb

[8] G. Gadhiya, B. Brämer, S. Rzepka, T. Otto. 22nd Europ. Microelectron. Packaging Conf. & Exhibition (EMPC), 19265124 (2019). DOI: 10.23919/EMPC44848.2019.8951805

[9] C. Ferrandon, B. KhoIti, L. Castagne, F. Casset, R. Franiatte, D. Mermin, G. Simon, G. Imbert, S. Petitdidier, F. Bailly, P. Chevalier, L. Toffanin, N. Chevrier, J.P. Pierrel. 6th Electron. System-Integration Technol. Conf. (ESTC), 16520083 (2016). DOI: 10.1109/ESTC.2016.7764485

[10] V.V. Gribko, A.S. Markelov, V.N. Trushin, E.V. Chuprunov. J. Surf. Investigation: X-Ray, Synchrotron and Neutron Techniques, **11** (3), 505 (2017). DOI: 10.1134/S1027451017030077

[11] V.V. Gribko, A.S. Markelov, V.N. Trushin, E.V. Chuprunov. Instruments and Experimental Techniques, **61** (1), 148 (2018). DOI: 10.1134/S0020441218010165

[12] V.V. Gribko, A.S. Markelov, V.N. Trushin, E.V. Chuprunov. Instruments and Experimental Techniques, **62** (5), 703 (2019). DOI: 10.1134/S0020441219040183

[13] E.B. Klyuenkov, V.N. Polkovnikov, N.N. Salashchenko, N.I. Chkhalo. Bull. Russ. Academy of Sciences: Physics, **72** (2), 188 (2008).

[14] N.N. Salashchenko, M.N. Toporov, N.I. Chkhalo. Bull. Russ. Academy of Sciences: Physics, **74** (1), 53 (2010). DOI: 10.3103/S1062873810010144

[15] A.A. Akhsakhalyan, A.D. Akhsakhalyan, S.A. Garakhin, N.N. Salashchenko, M.N. Toporov, N.I. Chkhalo, N.F. Erkhova, A.S. Kirichenko, S.V. Kuzin. Tech. Phys., **64** (11), 1680 (2019). DOI: 10.1134/S1063784219110033

[16] A.A. Akhsakhalyan, A.D. Akhsakhalyan, D.G. Volgunov, M.V. Zorina, M.N. Toporov, N.I. Chkhalo. Poverkhnost'. Rentgenovskie, sinkhrotronnye i nejtronnye issledovaniya, **7**, 93 (2015) (in Russian). DOI: 10.7868/S0207352815070033

[17] A.K. Chernyshev, I.V. Malyshev, A.E. Pestov, N.I. Chkhalo. Tech. Phys., **64** (11), 1560 (2019). DOI: 10.1134/S1063784219110069

[18] M.V. Zorina, I.M. Nefedov, A.E. Pestov, N.N. Salashchenko, S.A. Churin, N.I. Chkhalo. J. Surfa. Investigation: X-Ray, Synchrotron and Neutron Techniques, **9** (4), 765 (2015). DOI: 10.1134/S1027451015040394

[19] S.P. Radzevich. *Formoobrazovaniye poverkhnostei detalei (Osnovy teorii)* (Rastan, Kiev, 2001). (in Russian).

[20] S.Kh. Nguyen. Novaya Nauka: Sovremennoye sostoyanie i puti razvitiya, **12** (4), 99 (2016). (in Russian).

[21] B.B. Ponomarev, S.Kh. Nguyen. Vestnik Irkutskogo Gos. Tekh Un-ta, **22** (4), 62 (2018). (in Russian). DOI: 10.21285/1814-3520-2018-4-62-72

[22] X.L. Le, K. Kim, S.H. Choa. Intern. J. Precision Engineer. Manufactur., **23**, 347 (2022). DOI: 10.1007/s12541-021-00602-1

[23] V.S. Balderrama, J.A. Leon-Gil, D.A. Fernandez-Benavides, J. Ponce-Hernandez, M. Bandala-Sanchez. IEEE Sensors J., **22** (3), 1939 (2022). DOI: 10.1109/JSEN.2021.3135543

[24] R. Sharma, I. Yadav, A. Meena, M. Kumar, R. Saxena, K.K. Jain. Phys. Semicond. Dev., **215**, 855 (2019).

[25] C. Pollock, J. Morrison, M. Imboden, T.D.C. Little, D.J. Bishop. Opt. Express, **25** (17), 20274 (2017). DOI: 10.1364/OE.25.020274

[26] A.V. Krysko, J. Awrejcewicz, I.V. Papkova, V.A. Krysko. Materials, **13**, 3187 (2020). DOI: 10.3390/ma13143187

[27] A.A. Dedkova, I.V. Florinsky, N.A. Djuzhev. Proceed. SPIE — The Intern. Society for Opt. Engineer., 12157, 121571K (2022). DOI: 10.1117/12.2623908

[28] A.A. Dedkova, I.V. Florinsky, E.E. Gusev, N.A. Dyuzhev, M.Yu. Fomichev, M.Yu. Shtern. Russ. J. Nondestructive Testing, **57** (11), 1000 (2021). DOI: 10.1134/S1061830921110073

[29] A.A. Dedkova, I.V. Florinsky, N.A. Djuzhev. Phys. Usp., 65(7), 706 (2022). DOI: 10.3367/UFNe.2021.10.039076

[30] P.A. Shary, L.S. Sharaya, A.V. Mitusov. Geoderma, **107** (1/2), 1 (2002). DOI: 10.1016/S0016-7061(01)00136-7

[31] I.V. Florinsky, A.N. Pankratov. Intern. J. Geograph. Inform. Sci., **30** (12), 2506 (2016). DOI: 10.1080/13658816.2016.1188932

[32] A.A. Dedkova, P.Yu. Glagolev, E.E. Gusev, N.A. Dyuzhev, V.Yu. Kireev, S.A. Lychev, D.A. Tovarnov. ZhTF, **91** (10), 1454 (2021). (in Russian). DOI: 10.21883/JTF.2021.10.51357.121-21

[33] N.A. Djuzhev, E.E. Gusev, A.A. Dedkova, D.A. Tovarnov, M.A. Makhiboroda. Tech. Phys., **65** (11), 1755 (2020). DOI: 10.1134/S1063784220110055

[34] A.A. Dedkova, N.A. Dyuzhev, E.E. Gusev, M.Yu. Shtern. Russ. J. Nondestructive Testing, **56** (5), 452 (2020). DOI: 10.1134/S1061830920050046

[35] F. Zhao. Proceedings Modeling, Signal Processing, and Control for Smart Structures, **6926**, 69260W (2008). DOI: 10.1117/12.775511

[36] R.H. Plaut. Acta Mech., **202**, 79 (2009). DOI: 10.1007/s00707-008-0037-3

[37] J. Neggers, J.P.M. Hoenagels, F. Hild, S. Roux, M.G.D. Geers. Experimental Mechan., **54** (5), 717 (2014). DOI: 10.1007/S11340-013-9832-4

[38] L.E. Andreeva. *Uprugie elementy priborov* (Mashgiz, M., 1962) (in Russian)

[39] S.P. Timoshenko, S. Voynovsky-Kriger. *Plastiny i obolochki* (Nauka, M., 1966) (in Russian)

[40] G.G. Stoney. Proceed. Royal Society of London. Series A, **82** (553), 172 (1909). DOI: 10.1098/RSPA.1909.0021

[41] N.V. Filimonenkova, K.A. Danilova, P.N. Mironova. Aktualnye napravleniya nauchnykh issledovanii XXI veka: teoriya i praktika, **2** (4−1), 353 (2014). (in Russian). DOI: 10.12737/4778